Postprint of: N. A. Wójcik, B. Jonson, R. J. Barczyński, P. Kupracz, D. Möncke, S. Ali: Electrical properties of Na2O-CaO-P2O5 glasses doped with SiO2 and Si3N4. Solid State Ionics. Vol. 325 (2018), pp. 157-162. DOI: https://doi.org/10.1016/j.ssi.2018.08.011

Electrical properties of Na_2O-CaO-P_2O_5 glasses doped with SiO_2 and Si_3N_4

N. A. Wójcik[1,2*], B. Jonson[1], R. J. Barczyński[2], P. Kupracz[2], D. Möncke[1,3], S. Ali[1]

[1] *Department of Built Environment and Energy Technology, Linnæus University, 35195 Växjö, Sweden*

[2] *Department of Solid State Physics, Faculty of Applied Physics and Mathematics, Gdańsk University of Technology, Narutowicza Street 11/12, 80–233 Gdańsk, Poland*

[3] *Theoretical and Physical Chemistry Institute, National Hellenic Research Foundation, 48 Vassileos Constantinou Avenue, 11635 Athens, Greece*

**corresponding author:* natalia.wojcik@lnu.se; natalia.wojcik@pg.edu.pl

Abstract

Sodium-calcium-phosphate glasses doped with SiO_2 or Si_3N_4 having similar sodium ion concentrations were prepared by melt quenching. The conductivity was measured by impedance spectroscopy under nitrogen atmosphere in a wide frequency range (10 mHz – 1 MHz) and wide temperature range (153 - 473 K). At 36.6 °C, DC conductivities of all glasses vary between $1.1*10^{-12}$ and $8.9*10^{-12}$ Scm^{-1} and have similar activation energies (between 0.87 and 0.91 eV), which are characteristic for an ionic conduction mechanism. The analysis of AC conductivities showed that the spectra are governed by one dynamic process – hopping of the mobile charge carriers - which may be described i.e., by the ´concept of mismatch and relaxation` or by the `random barrier´ model. The obtained results confirmed a higher influence of nitrogen incorporation on the various glass conductivity parameters than shown for silicon doping alone. However, the influence of fundamental structural changes on the glass conductivity is less relevant as is the overall sodium ion concentration, which remains the decisive factor for a high ion conduction.

Keywords: Sodium-calcium-phosphate glasses, Oxynitride glass, Impedance spectroscopy

1. Introduction

Recently, the interest in phosphate glass research increased, mostly in regard to their application as bioactive materials [1-3]. The degradation rate and stability of glasses in the Na-Ca-P-O system can be controlled by silicon or nitrogen doping. In our previous work [4], we have shown that addition of low concentrations (1 - 2 mol%) of silicon oxide or silicon nitride causes significant changes in the Raman spectra of Na-Ca-P-O glasses. The thermal properties of the glasses e.g. glass transition and crystallization temperatures, thermal glass stability ($S = T_{exo} – T_g$) and fragility index

are also influenced by the Si_3N_4 content. A similar trend was observed for nitrogen rich silicon-based glasses [5-7]. Moreover, structural analysis of these glasses confirmed the presence of amorphous phosphates, which are likely to act as precursor for the crystallization of hydroxyapatites. Therefore, these materials are of great interest as potential bioactive glasses [8-10]. Usually, bioactive glasses exhibit not only good properties for diverse biomedical applications but due to their high sodium and calcium levels, these glasses are also good dielectrics. Nowadays, research focuses also on the fabrication of electrically conducting scaffolds made from bioactive glass-composites in order to stimulate cell growth electrically. It was shown that the construction of specific niches with conductive materials, such as conducting polymers, carbon nanotubes and graphene, can promote stem cell differentiation towards electro-active lineages and emphasize the promising role of stem cells in electro-active tissue regeneration [11, 12]. Moreover, Basset et al. [13] showed in the sixties, that when deformed, bones can produce electrical charges. Describing a relationship between piezoelectricity and callus formation, they also proposed that stress-induced bioelectric potentials control both bone cell activity and the orientation of their molecular bioproducts. Many researchers also found improvement in osteobonding and bone growth on the surface of polarized hydroxyl apatite (HA) after generating a permanent surface charge on the materials in vitro [14, 15].

However, the electrical processes that occur in bioactive materials were not further highlighted in these papers. Therefore, studying conduction processes in bioglasses is not only an exercise in fundamental research, but is also relevant for applications of said bioglasses.

The high sodium oxide content of bioactive glasses let us to expect a significant ionic conductivity for these glasses. Since conductivity is a property, which is sensitive to many effects, including small compositional and structural variations, we further expected significant variations in the electrical properties for the various Na-Ca-P-O glasses doped with low levels of SiO_2 and Si_3N_4, a system we have been studying earlier in detail in regard to glass formation, thermal properties and structural variations [4].

In the last decades, ionic conduction phenomena in different Na-containing glasses have attracted much interest even beyond the underlying fundamental mechanisms [16-19] but also for applications such as solid state batteries [20, 21]. One of the most common methods for studying charge carrier dynamics in disordered solids is

impedance spectroscopy. A detailed analysis of the frequency and temperature dependence of AC conductivity is necessary to characterize microscopic mechanisms of the charge carrier transport [18]. Several papers discuss the conductivity behavior of the Na-Si-O glass system containing different ions, including Ca^{2+} [16, 17, 22-24]. And while phosphorous-based glass systems have been extensively studied for mixed alkali [25] or mixed ion-polaron conduction effects [26-32], there is still a lack of fundamental knowledge regarding the electrical properties of the Na-Ca-P-O glass system, from which the important bioactive glasses derive.

The aim of this work is therefore to investigate the influence of a slightly changing glass matrix on the electrical properties of the Na-Ca-P-O glass system. Impedance studies are performed in order to analyze the influence of Si and N doping on the conductivity. Furthermore, the results of phosphorous-based glasses are compared with those of silicon-based glasses with a composition close to the well-known bioglasses: 45S5 ($44.97SiO_2$-$23.73Na_2O$-$26.23CaO$-$5.07PO_{5/2}$ in mol%) and S53P4 ($52.94SiO_2$-$22.28Na_2O$-$21.4CaO$-$3.38PO_{5/2}$ in mol%) [33].

2. Experimental

Four samples with approximately the same sodium content and different matrix composition were synthesized by the conventional melt quenching technique. First, the primary target glass 0P with a composition of $28.6Na_2O$-$14.3CaO$-$57.1PO_{5/2}$ (in mol%) was prepared from appropriate amounts of reagents: NaH_2PO_4 (≥ 99.5 % Sigma Aldrich), Na_2CO_3 (99.9 + % ChemPur GmbH) and $CaCO_3$ (99.9 + % ChemPur GmbH). Next, glasses (1PS) $1SiO_2$-$99(28.6Na_2O$-$14.3CaO$-$57.1PO_{5/2})$ and (2PSN) $2Si_3N_4$-$98(28.6Na_2O$-$14.3CaO$-$57.1PO_{5/2})$ (in mol%) were melted from shards of the pre-prepared target glass and reagent grade SiO_2 (99.99% ChemPur GmbH) or Si_3N_4 (ChemPur GmbH). Additionally, a silicon-based glass (3SP) $23.8Na_2O$-$19.1CaO$-$9.5PO_{5/2}$-$47.6SiO_2$ (in mol%), with similar sodium content was synthesised as a reference sample, having a similar composition as the well-known bioglasses 45S5 and S53P4. All samples were prepared in porcelain crucibles under air atmosphere. All samples are listed in Tab.1 with their ID, as analyzed compositions, and the respective melting process parameters. Similar trace amount of Al (~ 0.2 - 0.3 at%) from the crucibles are found in all samples and are not included in the nominal compositions of table 1. More detailed descriptions about the preparation process of these phosphate glasses can be found in reference [4]. Glass densities were measured

by the Archimedes method using ethylene glycol as an immersion fluid. The sodium-ion concentration (N_{Na+}) given as atoms cm^{-3} was calculated based on the measured densities and composition, according to relation:

$$N_{Na+} = \frac{d*n_{Na}*N_A}{M_{glass}} \qquad (1)$$

Where d is the glass density (in gcm^{-3}), M_{glass} is the molar mass of the glass (in $gmol^{-1}$), n_{Na} is the sodium ions content (in at%) and N_A is the Avogadro constant.

Plane parallel circular samples, polished on the surface were used for the electrical measurements. The diameter of the discs was approximately 10 mm and the glass thickness varied between 1 to 2 mm. In order to serve as electrodes, the glass discs were coated with gold, which was vaporized under vacuum. Impedance measurements were carried out in the frequency range from 10 mHz to 1 MHz in a temperature range of 153 K to 473 K, with an AC voltage of 1 V_{rms} using a Novocontrol Concept 40 broadband dielectric spectrometer. The measurements were conducted under nitrogen atmosphere. Using a dielectric analyzer, only spectra with a conductivity from 10^{-14} Scm^{-1} or more can be recorded, thus, only results taken above 213 K could be effectively analyzed.

3. Results and discussion

In order to discuss the electrical properties of the prepared glasses, it is worth to compare these properties also with the thermal properties and the structure of each of the studied glasses. A thorough discussion on glass formation and on structure property correlation in the Na-Ca-P-O-N glass system can be found in detail in our previous paper [4] and only results most important for the current study will be briefly summarized in the following paragraph.

All obtained glasses were homogeneous and amorphous. Glasses 0P, 1PS and 2PSN contained ~18 at% of sodium or ~$1.3*10^{22}$ $atoms*cm^{-3}$ (Tab. 1), which resulted in a high degree of depolymerization. The addition of small quantities of silicon oxide (glass 1PS) or silicon nitride (glass 2PSN) caused significant changes in the Raman spectra. For 0P, as expected from the composition, 50% of the phosphate tetrahedra form Q^2 units or $(PO_{2/2}O_2)^-$ that is, phosphate tetrahedra with 2 bridging and 2 terminal

oxygen atoms, and the other 50% consisted of Q^1 units, $PO_{1/2}O_3^{2-}$. The phosphate structure in glasses 1PS and 2PSN however was significantly more depolymerized with signatures of Q^1 units dominating in the Raman spectra. This was explained by six-fold coordinated silicon, as special case, though typical when low levels of silicate are dissolved in phosphate glasses where each Si-atom connects to 6 PO_4-tetrahedra [35]. In its high coordination form, SiO_2 acts more like a network modifier than a network former, depolymerizing the glass network. 3SP was not part of the previous study, but with a composition of $23.8Na_2O$-19CaO-$9.5PO_{5/2}$-$47.6SiO_2$ (in mol%), has the fraction of modifier oxides similar to the three phosphate glasses of this study. 3SP is a metasilicate based glass containing "isolated" orthophosphate units [34].

Thermal analysis showed that the addition of low Si and N concentrations increases the glass transition temperature T_g by more than 80 °C whereas values for the thermal glass stability S, increase only slightly. The glass 3SP shows significantly higher T_g (537 °C) and lower S (129 °C) values than phosphate glasses, but has a slightly lower transition temperature than the well-known bioglasses: 45S5 (T_g = 552 °C) and S53P4 (T_g = 561 °C) [33].

Table 1 Studied glasses with their corresponding glass compositions (as analyzed), melting process parameters: temperature ($T_{melting}$) and time ($t_{melting}$), density and sodium-ion concentration.

Samples ID	Comment	Measured composition (wt%) +/- 5%	Measured composition (at%) +/- 5%	$T_{melting}$ (°C)	$t_{melting}$ (min)	Density (gcm^{-3}) +/- 0.01	*Na^+ concentration (cm^{-3})* +/- 5%
0P	Target glass	$Na_{20.4}Ca_{9.4}P_{24.6}O_{45}$	$Na_{18.5}Ca_5P_{16.8}O_{59.5}$	950	30	2.61	$1.38*10^{22}$
1PS	Si doped glass	$Na_{20.1}Ca_{8.5}P_{25.3}Si_{0.5}O_{45}$	$Na_{18.2}Ca_{4.5}P_{17.3}Si_{0.4}O_{59.4}$	1000	30	2.60	$1.35*10^{22}$
2PSN	Si and N doped glass	$Na_{19.1}Ca_{8.7}P_{24.5}Si_{1.7}O_{44.3}N_{1.4}$	$Na_{17.3}Ca_{4.6}P_{16.6}Si_{1.3}O_{58}N_{2.1}$	1300	20	2.55	$1.26*10^{22}$
3SP	Reference glass	$Na_{19.7}Ca_{12.2}P_{5.2}Si_{21.2}O_{41.7}$	$Na_{18.3}Ca_{6.5}P_{3.6}Si_{16.1}O_{55.5}$	1350	30	2.57	$1.29*10^{22}$

Figure 1a shows for all prepared glasses the real part of conductivity (σ´) versus the temperature as measured at three different frequencies. The σ´ values of the glasses increase with temperature and frequency. The conductivity values are of the same order of magnitude, when comparing glasses that were measured under the same conditions (specific temperature and frequency). In Figure 1b, the frequency dependence of σ´ is plotted for different temperatures on the example of glass 3SP. The other glasses show similar tendencies of their σ´ curves. The conductivity spectra can be divided into two parts: the frequency-independent DC conductivity (σ_{DC}) and

the AC conductivity, which increases with frequency. The frequency range of the DC plateau increases with the temperature for all studied samples.

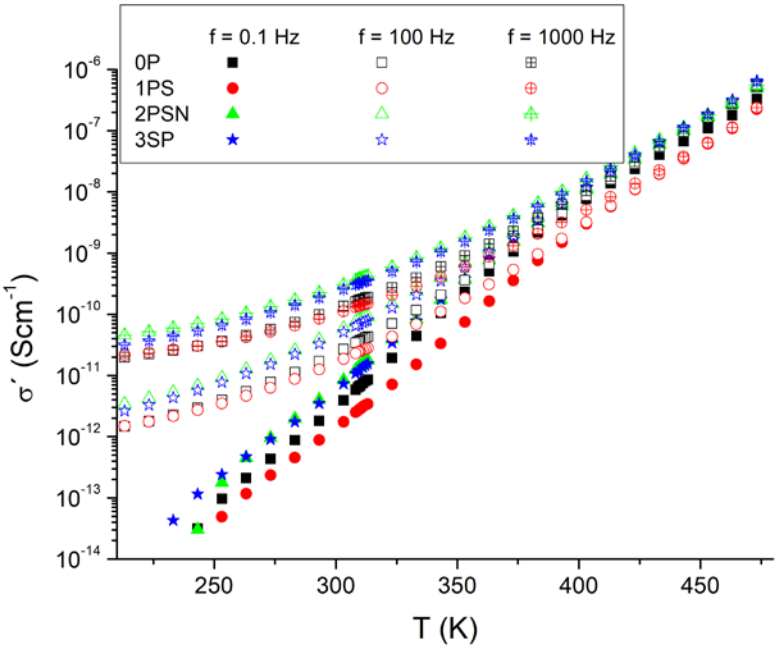

(a)

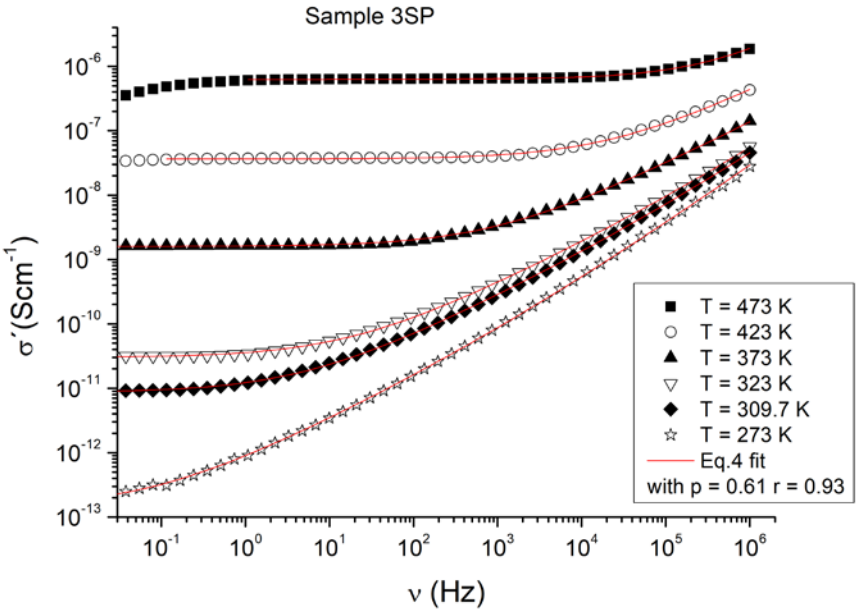

(b)

Figure 1 (a) Real part of conductivity as a function of temperature for three different frequencies (symbol filling) shown for all samples (symbol form). **(b)** Frequency dependence of the real part of conductivity for glass 3SP plotted for six different temperatures. The red lines show the fit using Eq. 4.

The σ_{DC} values (obtained from Fig.1b) are presented in Fig. 2 as crossed symbols. They obey the Arrhenius law which is given by equation (2), over a conductivity range of more than seven magnitudes.

$$\sigma_{DC}T \sim e^{-\frac{E_A}{kT}} \qquad (2)$$

The E_A activation energy is related to a fundamental migration step in the conduction process [35]. The straight lines in Fig. 2 show the fit results for the Arrhenius relation. Values for the activation energy E_A and the frequency-independent DC conductivity σ_{DC} (at 36.6 ^{o}C) are listed in Tab. 2. For all glasses, σ_{DC} values vary between $1.1*10^{-12}$ and $8.9*10^{-12}$ Scm^{-1}. The glass 1PS doped with 0.4 at% of silicon, shows the lowest value of σ_{DC} with the highest activation energy 0.95 eV, while glass 2PSN containing 1.3 at% of silicon and 2.1 at % of nitrogen exhibits the highest σ_{DC} with the lowest E_A = 0.86 eV. However, glass 3SP, despite having a silicate rather than a phosphate based glass matrix, exhibits values of DC conductivity and E_A that are almost the same as those of the glass 2PSN. The activation energy magnitude observed is typical for an ion hopping mechanism [24] and we can therefore conclude that Na^+ hopping is the ion conduction mechanism in our glasses.

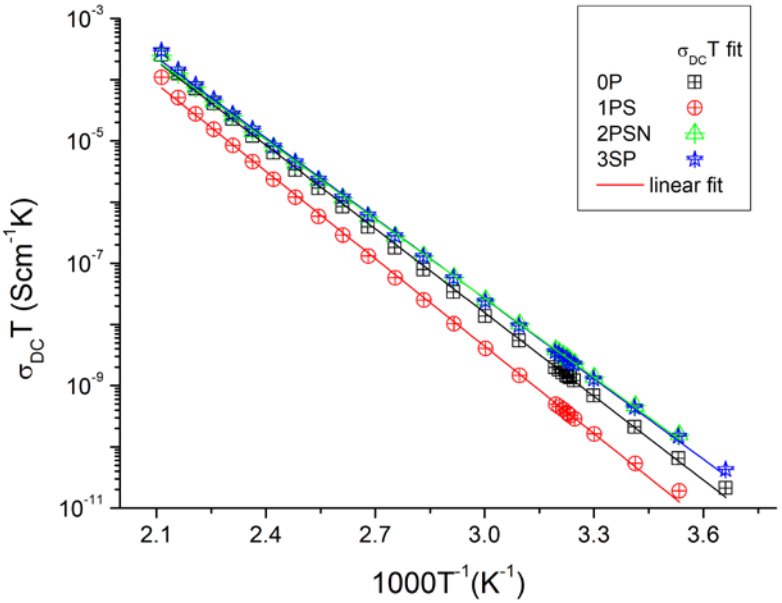

Figure 2 Arrhenius plot of the DC conductivity of all glasses. The straight lines show the results of the Arrhenius fit (Eq. 2).

Table 2 Conductivity parameters: σ_{DC} (from Fig. 1b), E_A of DC conductivity process (fit of Arrhenius relation of data from Fig. 2), exponents *p* and *r*, frequencies ν_J and ν_{NCL} (fitting data in Fig. 3 with Eq. 4), and *slope* (linear fit to data in Fig. 4). For further information see also description in the text.

Glass ID	E_A (σ_{DC}) (eV) +/- 0.01	σ_{DC} at 36.6 °C (Scm^{-1}) +/- 0.01	*p* +/- 0.01	$\nu_J(\sigma_{DC}T)^{-1}$ ($HzcmS^{-1}K^{-1}$)	*r* +/- 0.01	$\nu_{NCL}(\sigma_{DC}T)^{-1}$ ($HzcmS^{-1}K^{-1}$)	*slope* +/- 0.01
0P	0.91	$4.57*10^{-12}$	0.59	$2.52*10^{9}$	0.95	$1.12*10^{11}$	1.11
1PS	0.95	$1.12*10^{-12}$	0.60	$1.77*10^{9}$	0.95	$9.34*10^{10}$	1.07
2PSN	0.86	$8.89*10^{-12}$	0.56	$8.40*10^{8}$	0.93	$3.69*10^{10}$	1.05
3SP	0.87	$8.41*10^{-12}$	0.61	$1.58*10^{9}$	0.93	$6.11*10^{10}$	1.10

DC and AC conduction are both governed by the same mechanism and are connected with each other. Therefore, a proper understanding of AC conduction is also important in order to obtain an in depth picture of ion transport mechanisms [36]. AC conductivity of many dielectric systems can be described by the Jonscher power law expressed by the following relation:

$$\sigma'(\vartheta) = \sigma_{DC}\left[1 + \left(\frac{\vartheta}{\vartheta_J}\right)^p\right] \qquad (3)$$

Where ν_J is the onset frequency of the conductivity dispersion, exhibiting an Arrhenius-type temperature dependence. The exponent *p* is usually smaller than unity [37]. However, at high frequencies and/or low temperatures (where the frequency ν exceeds ν_J by several orders of magnitude), the exponent achieves a value that equals 1. This type of frequency response is known as “nearly constant loss” (NCL) because of the negligible frequency dependence of the dielectric function $\varepsilon''(\vartheta) = \frac{\sigma'(\vartheta)}{2\pi\vartheta\varepsilon_0}$ [18].

Nowick [38] proposed to describe the entire AC conductivity spectra of ion-conducting glasses by superimposing the Jonscher relation with the NCL term:

$$\sigma'(\upsilon) = \sigma_{DC}[1 + \left(\frac{\upsilon}{\upsilon_J}\right)^p + \left(\frac{\upsilon}{\upsilon_{NCL}}\right)^r] \qquad (4)$$

Where exponent *r* is equal 1 and ν_J, ν_{NCL} depend on the number density of the mobile particles, the jump distance and temperature. Based on the results of equation *(4)* some authors state that Jonscher and NCL behavior originate from clearly distinct dynamic processes. In their opinion, the first process is due to subdiffusive and diffusive hopping motions of mobile ions whereas the NCL process is often attributed

to the motion of groups of atomic species, including mobile charge carriers and network atoms, an asymmetric double-well potential (ADWP) configurations [39-42].

Dyre et al. [43] reviewed the AC characteristics of many disordered solids. They have noticed that at high frequencies, σ´(ω) follows indeed an apparent power law. However, the power-law exponent increases slightly with the frequency and is found to be between 0.6 and 1.0. In a fixed frequency range the exponent increases as the temperature decreases with $n \rightarrow 1.0$ for $T \rightarrow 0$. These observations are in disagreement with equation *(4)*, which does not predict any increase of the exponent with frequency.

However, there are other models describing ion dynamics in glasses, which indeed predict all above mentioned characteristics, for instance, the `concept of mismatch and relaxation` (CMR) proposed by Funke [44] or the `random barrier model` (RBM) described by Dyre [36, 43, 45]. Both mentioned models describe the entire AC conductivity spectra by the hopping dynamics of the mobile charge carriers. Roling et al. [18] have shown that the hopping dynamics of mobile ions lead in various ion conducting glasses above the temperature of 100 K, to AC conductivities and that the formal separation into distinct power-law regimes (Jonscher and NCL) may be artificial. In this work, we are conducting a similar route of analysis as stated in reference [18] in order to determine if the entire AC conductivity spectra - for all measured temperature ranges and all glasses presented here - can equally be described only by hopping motions of the mobile ions.

It is known that the AC conductivity obeys time-temperature superposition, i.e., the shape of σ´(ω) in log-log plot is temperature independent and it is possible to construct a master curve [43]. Figure 3a presents the master curve of the AC conductivity spectra of glass 2PSN. This master curve was generated by plotting $\sigma'\sigma_{DC}^{-1}$ vs. $\nu(\sigma_{DC}T)^{-1}$. Any spectra with detectable σ_{DC} were observed only for temperatures above 263 K (Fig. 1b), for which the master curve extends over approximately 6 orders of magnitude on the $\sigma'\sigma_{DC}^{-1}$ plot. Master curves of the AC conductivity spectra were obtained analogously for other glasses.

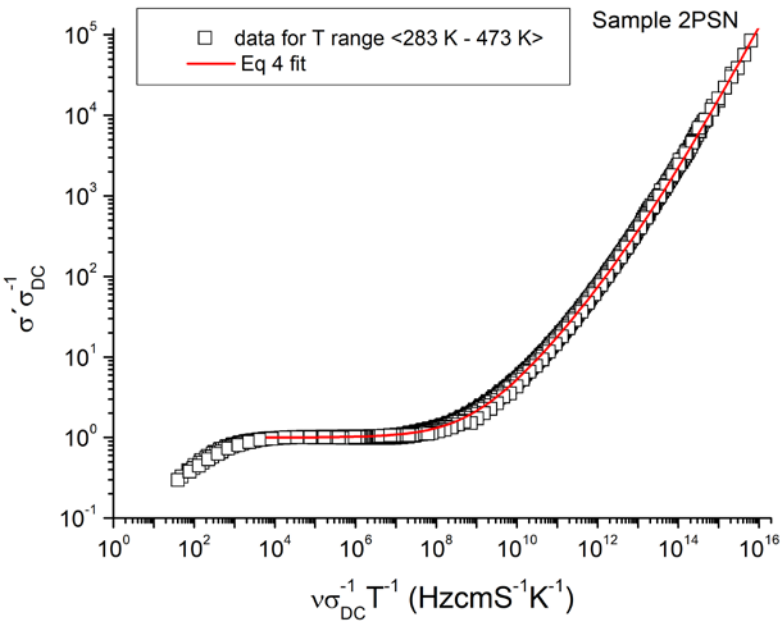

Figure 3 Master curve of AC conductivity of glass 2PSN.

The slope of d logσ´/ d logν continuously increases from ~0.56 in the Jonscher regime up to ~0.95 in the NCL regime, for all glasses investigated. This increase of the conductivity slope with frequency is in disagreement with equation *(4),* as previously noticed by Dyre et al. [43]. However, to examine the interrelation between Jonscher and NCL behavior, we intentionally use Eq. 4 to estimate the approximate values of frequencies ν_J and ν_{NCL}. Firstly, we fit the Eq. 4 to the master curves (Fig. 3), which resulted in apparent exponents and frequencies independent of temperature as listed in table 2. The values of the apparent slopes *p* and *r* (from Tab. 2) were used to fit Eq. 4 to the conductivity spectra in Fig. 1b. These fit results are marked by red lines and fit the conductivity data very well for all glasses at all temperatures. However, the AC conductivity spectral shapes predicted by the RBM [36] and CMR [44] models may be just as easily fitted by Eq. 4 and, contrary to Equation 4, predict these models actually the continuous increase of the apparent exponent of conductivity with increase in frequency.

The fit of Eq. 4 to AC conductivity spectra (Fig. 1b) gives the values of frequencies ν_J and ν_{NCL}, which are shown for all glasses in Fig. 4 using the log-log scale. The linear relation between frequencies ν_J and ν_{NCL} for our glasses confirms the close interrelation between the Jonscher and the NCL behavior. The straight lines in Fig. 4 show the linear fit results and the values of their *slopes* are listed in Tab.2. The slopes are close

to one. These results are in agreement with the RBM model and the observations made by Roling et al. [18]. Therefore, we may conclude that in all our glasses in the presented temperature and frequency range, AC conductivity spectra are due to one dynamic process – hopping of the mobile ion – Na^+.

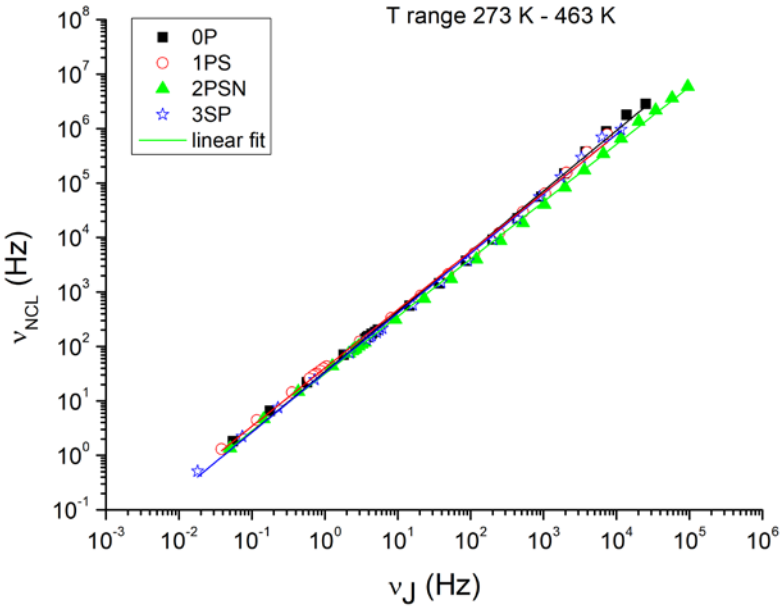

Figure 4 Characteristic frequencies ν_{NCL} versus ν_J for all glasses estimated from Eq. 4 fit to conductivity spectra in Fig. 1b

The interpretation of the observed differences of the conductivity parameters for the various glasses investigated, will also be based on structural findings presented in our previous paper [4]. There, we showed that glasses doped with SiO_2 and Si_3N_4 exhibit less polymerized networks than was initially present in the glass 0P. The increase in depolymerization of the modified glasses was caused by the uptake of modifier oxides from the crucible material (Al_2O_3 and Na_2O) as well as the addition of SiO_2 which is known to be octahedrally coordinated when present as minor component in phosphate glasses [46]. Thus, all these additions will increase the number of non-bridging oxygen atoms in the phosphate network from a Q^1:Q^2 ratio of 1:1 in glass 0P, to a predominance of Q^1 over Q^2 in 1PS and 2PSN. Since the observed depolymerization of the phosphate network derives from the incorporation of SiO_2, Al_2O_3 and Nb_2O_5, all containing highly charged cations, remains the absolute number of potential mobile Na^+ ions of similar magnitude or decreases even slightly in the two

modified phosphate glasses. The slight decrease in n_{Na+} cm^3 cannot explain the significant drop in σ_{DC} for the glass 1PS (to almost a quarter of 0P), and on the side the doubling in a σ_{DC} for glasses 2PSN and 3SP. Similarly, E_A is higher for 1PS and lower for 2PSN and 3SP compared to glass 0P. It seems that the structural modifications have a strong impact on the mobility of the Na^+ ions.

As mentioned earlier, the role of SiO_2 is different when it acts as minor or major component in a silico-phosphate glass. As minor component, Si^{4+} is linked to 6 phosphate units, see for example Venkatachalam et al. [35], as major component silicate tetrahedra connect to shape the glass network. Depending on the modifier oxide concentration, non-bridging oxygen form on the phosphate tetrahedra, but not on octahedral coordinated silicate. Comparing glasses 0P and 1PS, the observed difference in activation energy and conductivity is most likely linked to a mixed modifier effect or a mixed network former effect, depending on the classification of highly charged Al^{3+} ions in tetrahedral and Si^{4+} ions in octahedral coordination as network modifier or former.

Glass 2PSN was prepared under similar conditions as glass 1PS, only that Si_3N_4 was doped instead of SiO_2. The silicon content is even higher than in glass 1PS, and additionally contains glass 2PNS also nitrogen. However, this glass exhibits a higher conductivity than both glasses 0P and 1PS. This phenomenon was observed in several oxynitride glass systems [47-50]. One explanation given for the increase in ionic conductivity is the decreasing electrostatic energy of the glass network resulting from nitrogen incorporation.

In this context, let us briefly consider the effects of the electrostatic binding energy E_b and network strain energy E_s on ion conduction. E_b describes the coulombic forces acting on the ion as it moves away from its charge-compensating site, and E_s describes the mechanical forces acting on the ion as it dilates the structure sufficiently to allow the ion to move between sites [51]. As P-O bonds are replaced by more covalent P-N bonds, the increase of network strain energy could be counteracted, leading to an effective decrease of E_A [52, 53]. This suggestion is in accordance with the Anderson-Stuart model, which establishes that the activation energy of ionic conduction depends on two terms, i.e. the network strain energy and the change of electrostatic bonding energy of the original site [46].

In the present work, by comparing the two re-melted glasses 1PS and 2PSN, it is shown that the influence of nitrogen incorporation on glass conductivity is high enough to compensate the impeding effect of silicon doping.

When comparing the conductivity parameters of the three phosphate glasses with the 3SP silicate glass containing a similar sodium-ion concentration (~$1.3*10^{22}$ cm^{-3}, Tab.1) it is observed that the electrical properties, especially between glass 2PSN and glass 3SP, are very similar, despite changing from a phosphate based to a silicate based glass matrix.

Like phosphate glasses, silicate glass consists of glass forming tetrahedra. However, the role of the minority phosphate component in a silicate glass is very different to Si as minor addition in a phosphate glass. In silico-phosphate glasses, octahedrally coordinated silicate is bonded to 6 phosphate tetrahedra, while in phosphor-silicate glasses, orthophosphate tetrahedra are not linked directly to the silicate network [34]. It seems, that the mixed network modifier/former effect is less pronounced in this second type of more open structural arrangements with non-bridging oxygen ions, while centered at orthophosphate units, are also distributed over all silicate tetrahedra. On the other hand, when SiO_2 acts as modifier, the Si^{4+} ions charge balancing 6 terminal oxygen ions on phosphate tetrahedra [54], ion conduction of mobile ions is impeded by the presence of these lager superstructural units.

Overall, considering the similar conductivities and activation energies of all 4 glasses studied, the differences we observed due to the structural changes between these glasses are relatively small. Much stronger variations in conductivities and activation energies, covering several orders of magnitude, are observed in systems with much higher sodium ion concentration [51]

Conclusions

Sodium-calcium-phosphate glasses doped with SiO_2 or Si_3N_4 as well as a silicate-based glass were prepared in such a way, that they all contained similar Na concentration. Analysis of the electrical properties showed that for all the prepared glasses DC conductivity values vary between $1.1*10^{-12}$ and $8.9*10^{-12}$ Scm^{-1}. The activation energy of DC conductivity varies between 0.86 eV for the glass containing silicon and nitrogen to 0.95 eV for the glass doped only with silicon. The analysis of AC conductivity showed that the spectra are governed by one dynamic process –

hopping of the mobile charge carriers, which may be described by for instance, the `random barrier model` or the `concept of mismatch and relaxation`. The predominant process in DC and AC conduction in all measured glasses is sodium ion hopping.

It is shown that the influence of nitrogen incorporation on glass conductivity parameters is high enough to compensate the negative impact of the mixing effect due to silicon incorporation in silico-phosphate glasses, where octahedral coordinated Si^{4+} links phosphate entities to larger units. A similar negative mixed cation effect is negligible in phospho-silicate glasses, where tetrahedral orthophosphate is not directly linked to the network forming silicate tetrahedral.

However, the quite similar electrical properties of all phosphate glasses and of silicate glass with significantly different glass matrix, led to conclusion that the impact of structural variations on the glasses' conductivity is not as prevalent as the sodium ion concentration.

Acknowledgements

SA, BJ and NW acknowledge the financial support from the Crafoord Foundation (Grant No: 20160900). SA also acknowledge support from the Vinnova (Grant No. 2015-04809) and the ÅForsk Foundation (Grant No. 14-457).

DM thanks the Knowledge Foundation for financing her stay at Linnaeus University (Grant No 68110029).

References

[1] E.A. Abou Neel, D.M. Pickup, S.P. Valappil, R.J. Newport, J.C. Knowles, *J. Mater. Chem.* **19** (2009) (6) 690.
[2] A.V. Gayathri Devi, V. Rajendran, N. Rajendran, *International Journal of Engineering Science and Technology* **2** (2010) (6) 2483.
[3] A.R. Boccaccini, D.S. Brauer, L. Hupa, *Bioactive Glasses: Fundamentals, Technology and Applications*, Royal Society of Chemistry (2016).
[4] N.A. Wójcik, B. Jonson, D. Möncke, D. Palles, E.I. Kamitsos, E. Ghassemali, S. Seifeddine, M. Eriksson, S. Ali, *Journal of Non-Crystalline Solids* **494** (2018) 66.
[5] S. Ali, B. Jonson, *J. Eur. Ceram. Soc.* **31** (2011) (4) 611.
[6] S. Ali, J. Grins, S. Esmaeilzadeh, *Journal of Non-Crystalline Solids* **355** (2009) (4-5) 301.
[7] S. Ali, J. Grins, S. Esmaeilzadeh, *Journal of the European Ceramic Society* **28** (2008) (14) 2659.
[8] J.R. Jones, *Acta Biomater* **9** (2013) (1) 4457.
[9] T. Kokubo, *Biomaterials* **12** (1991) (2) 155.
[10] R.Z. LeGeros, *Clin Orthop Relat R* (2002) (395) 81.
[11] M. Turk, A.M. Deliormanli, *J Biomater Appl* **32** (2017) (1) 28.
[12] H. Porwal, S. Grasso, L. Cordero-Arias, C.C. Li, A.R. Boccaccini, M.J. Reece, *J Mater Sci-Mater M* **25** (2014) (6) 1403.

[13] C.A. Bassett, R.J. Pawluk, R.O. Becker, *Nature* **204** (1964) 652.
[14] S. Tigunta, N. Pisitpipathsin, P. Kantha, S. Eitssayeam, G. Rujijanagul, T. Tunkasiri, K. Pengpat, *Ferroelectrics* **459** (2014) (1) 188.
[15] T. Kobayashi, S. Nakamura, K. Yamashita, *J Biomed Mater Res* **57** (2001) (4) 477.
[16] H. Mehrer, A.W. Imre, E. Tanguep-Nijokep, *Journal of Physics: Conference Series* **106** (2008).
[17] B. Roling, M.D. Ingram, *J. Non-Cryst. Solids* **265** (2000) 113.
[18] B. Roling, C. Martiny, S. Murugavel, *Phys. Rev. Lett.* **87** (2001) (8) 085901.
[19] B. Roling, C. Martiny, S. Brückner, *Physical Review B* **63** (2001) (21).
[20] T. Masahiro, H. Akitoshi, *International Journal of Applied Glass Science* **5** (2014) (3) 226.
[21] M. Jamal, G. Venugopal, M. Shareefuddin, M. Narasimha Chary, *Materials Letters* **39** (1999) (1) 28.
[22] N. Pisitpipathsin, P. Kantha, S. Eitsayeam, G. Rujijanakul, R. Guo, A.S. Bhalla, K. Pengpat, *Integrated Ferroelectrics* **142** (2013) (1) 144.
[23] F.M.E. Eldin, N.A. El Alaily, *Mater. Chem. Phys.* **52** (1998) (2) 175.
[24] M.L. Braunger, C.A. Escanhoela, I. Fier, L. Walmsley, E.C. Ziemath, *J. Non-Cryst. Solids* **358** (2012) (21) 2855.
[25] R.F. Bartholomew, *J. Non-Cryst. Solids* **12** (1973) (3) 321.
[26] P. Jozwiak, J.E. Garbarczyk, M. Wasiucionek, I. Gorzkowska, F. Gendron, A. Mauger, C. Julien, *Mater Sci-Poland* **27** (2009) (1) 307.
[27] A. Moguš-Milanković, A. Šantić, A. Gajović, D.E. Day, *J. Non-Cryst. Solids* **296** (2001) (1) 57.
[28] R.S.D. Oliveira, J.A.C.D. Paiva, M.A.B.D. Araujo, A.S.B. Sombra, *Il Nuovo Cimento D* **20** (1998) (2) 209.
[29] L. Murawski, R.J. Barczynski, D. Samatowicz, *Solid State Ionics* **157** (2003) (1-4) 293.
[30] R.J. Barczynski, *Opt Appl* **35** (2005) (4) 875.
[31] R.J. Barczynski, L. Murawski, *J. Non-Cryst. Solids* **307** (2002) 1055.
[32] R.J. Barczynski, P. Krol, L. Murawski, *J. Non-Cryst. Solids* **356** (2010) (37-40) 1965.
[33] J. Massera, S. Fagerlund, L. Hupa, M. Hupa, *J. Am. Ceram. Soc.* **95** (2012) (2) 607.
[34] A. Pedone, T. Charpentier, G. Malavasi, M.C. Menziani, *Chemistry of Materials* **22** (2010) (19) 5644.
[35] A.S. Nowick, A.V. Vaysleyb, W. Liu, *Solid State Ionics* **105** (1998) (1-4) 121.
[36] J.C. Dyre, *J. Appl. Phys.* **64** (1988) (5) 2456.
[37] A.K. Jonscher, *Nature* **267** (1977) (5613) 673.
[38] W.K. Lee, J.F. Liu, A.S. Nowick, *Phys. Rev. Lett.* **67** (1991) (12) 1559.
[39] A.S. Nowick, B.S. Lim, A.V. Vaysleyb, *J. Non-Cryst. Solids* **172** (1994) 1243.
[40] A.S. Nowick, B.S. Lim, *Journal of Non-Crystalline Solids* **172** (1994) 1389.
[41] H. Jain, X. Lu, *Journal of Non-Crystalline Solids* **196** (1996) 285.
[42] H. Jain, X.D. Lu, *J Am Ceram Soc* **80** (1997) (2) 517.
[43] J.C. Dyre, T.B. Schroder, *Rev. Mod. Phys.* **72** (2000) (3) 873.
[44] K. Funke, D. Wilmer, *Solid State Ionics* **136** (2000) 1329.
[45] T.B. Schroder, J.C. Dyre, *Phys. Rev. Lett.* **101** (2008) (2).
[46] O.L. Anderson, D.A. Stuart, *J. Am. Ceram. Soc.* **37** (1954) (12) 573.
[47] A. Kidari, M.J. Pomeroy, S. Hampshire, *J. Eur. Ceram. Soc.* **32** (2012) (7) 1389.
[48] A. Kidari, C. Mercier, A. Leriche, B. Revel, M.J. Pomeroy, S. Hampshire, *Materials Letters* **84** (2012) 38.
[49] N. Mascaraque, J.L.G. Fierro, A. Durán, F. Muñoz, *Solid State Ionics* **233** (2013) 73.
[50] B. Wang, B.S. Kwak, B.C. Sales, J.B. Bates, *J. Non-Cryst. Solids* **183** (1995) (3) 297.
[51] M.L.F. Nascimento, *Journal of Materials Science* **42** (2007) (11) 3841.
[52] H. Unuma, K. Komori, S. Sakka, *J. Non-Cryst. Solids* **95-6** (1987) 913.
[53] H. Unuma, S. Sakka, *J. Mater. Sci. Lett.* **6** (1987) (9) 996.
[54] S. Venkatachalam, C. Schröder, S. Wegner, L. van Wüllen, *Physics and Chemistry of Glasses - European Journal of Glass Science andTechnology Part B* **55** (2014) (6) 280.